

Optical Coherence Tomography: Advanced Technology for the Endoscopic Imaging of Barrett's Esophagus

X. D. Li¹, S. A. Boppart^{1,2}, J. Van Dam³, H. Mashimo^{4,5}, M. Mutinga⁶, W. Drexler¹, M. Klein⁷, C. Pitris^{1,2}, M. L. Krinsky⁴, M. E. Brezinski⁵, J. G. Fujimoto¹

¹ Dept. of Electrical Engineering and Computer Science, Research Laboratory of Electronics, Massachusetts Institute of Technology, Cambridge, Massachusetts, USA

² Harvard-MIT Division of Health Sciences and Technology, Cambridge, Massachusetts, USA

³ Gastroenterology Division, Stanford University Medical Center, Stanford, California, USA

⁴ Gastroenterology Division, West Roxbury VA Medical Center, West Roxbury, Massachusetts, USA

⁵ Dept. of Medicine, Massachusetts General Hospital, Harvard Medical School, Boston, Massachusetts, USA

⁶ Gastroenterology Division, Brigham and Women's Hospital, Harvard Medical School, Boston, Massachusetts, USA

⁷ Dept. of Pathology, West Roxbury VA Medical Center, West Roxbury, Massachusetts, USA

Background and Study Aims: Endoscopic optical coherence tomography (OCT) is an emerging medical technology capable of generating high-resolution cross-sectional imaging of tissue microstructure in situ and in real time. We assess the use and feasibility of OCT for real-time screening and diagnosis of Barrett's esophagus, and also review state-of-the-art OCT technology for endoscopic imaging.

Materials and Methods: OCT imaging was performed as an adjunct to endoscopic imaging of the human esophagus. Real-time OCT (13- μm resolution) was used to perform image-guided evaluation of normal esophagus and Barrett's esophagus. Beam delivery was accomplished with a 1-mm diameter OCT catheter-probe that can be introduced into the accessory channel of a standard endoscope. Different catheter-probe imaging designs which performed linear and radial scanning were assessed. Novel ultrahigh-resolution (1.1- μm resolution) and spectroscopic OCT techniques were used to image in vitro specimens of Barrett's esophagus.

Results: Endoscopic OCT images revealed distinct layers of normal human esophagus extending from the

epithelium to the muscularis propria. In contrast, the presence of gland- and crypt-like morphologies and the absence of layered structures were observed in Barrett's esophagus. All OCT images showed strong correlations with architectural morphology in histological findings. Ultrahigh-resolution OCT techniques achieved 1.1- μm image resolution in in vitro specimens and showed enhanced resolution of architectural features. Spectroscopic OCT identified localized regions of wavelength-dependent optical scattering, enhancing the differentiation of Barrett's esophagus.

Conclusions: OCT technology with compact fiberoptic imaging probes can be used as an adjunct to endoscopy for real-time image-guided evaluation of Barrett's esophagus. Linear and radial scan patterns have different advantages and limitations depending upon the application. Ultrahigh-resolution and spectroscopic OCT techniques improve structural tissue recognition and suggest future potential for resolution and contrast enhancements in clinical studies. A new balloon catheter-probe delivery device is proposed for systematic imaging and screening of the esophagus.

Introduction

Biopsy and histopathological examination are the standard for the diagnosis of carcinoma, but can suffer from sampling errors and are cumbersome for wide-scale screening. A technology capable of performing "optical biopsy," imaging tissue at a resolution comparable to histopathological examination in situ and in real time, without the need for tissue removal and processing, could significantly improve the detection of malignancies. The imaging of tissue archi-

tectural morphology such as the integrity of the basement membrane and glandular organization could be used to detect many dysplastic and neoplastic changes.

Optical coherence tomography (OCT) is an emerging medical imaging technology which can perform high-resolution (1–15- μm) cross-sectional imaging of tissue microstructure in situ and in real time [1,2]. Several features of OCT, in addition to its high resolution, make it especially promising for medical diagnostics. In contrast to conventional optical imaging modalities, OCT provides cross-sectional images of internal tissue pathology, similarly to histopathology. Although OCT images do not have the resolution of histological techniques, OCT can perform imaging of tissue in situ, enabling larger areas of tissue to be exam-

ined than by excisional biopsy. Furthermore, OCT imaging can be performed in real time under operator guidance. Thus, OCT may be used to guide conventional excisional biopsy or interventional procedures. The electronic format of OCT images is directly amenable to computer image-processing techniques to enhance image quality as well as to quantify diagnostically relevant information. Since OCT is an optical technique, spectroscopic techniques using different wavelengths may be used to enhance tissue contrast or to perform microstructural functional assessment. Finally, unlike ultrasound, OCT imaging can be performed directly through air, avoiding the need for direct contact with tissue or the requirement of a transducing media. OCT can be easily interfaced with endoscopes, laparoscopes, catheters, and hand-held probes. Unlike magnetic resonance imaging or computed tomography, OCT can be engineered into a compact, portable, and relatively inexpensive instrument, allowing wider accessibility for possible office-based screening.

OCT was initially applied for imaging in the eye and, to date, has had the largest clinical impact in ophthalmology [3–5]. More recently, advances in OCT technology have made it possible to image nontransparent tissues, thus enabling OCT to be applied in a wide range of medical specialties [6–9]. Imaging depth is limited by optical attenuation from tissue scattering and absorption, but depths approaching 2–3 mm can be achieved in most tissues, comparable to depths obtained by conventional biopsy and histological investigation. Although imaging depths are limited, the resolution of OCT is 1–15 μm , i.e. 10 to 100 times finer than even high-resolution clinical ultrasound.

Numerous *in vitro* imaging studies have been performed, including studies of gastrointestinal tissues [10–14]. OCT has been interfaced with catheters, endoscopes, and laparoscopes that permit internal body imaging [15–19]. Catheter and endoscope OCT imaging of the gastrointestinal and pulmonary tracts has been demonstrated *in vivo* in an animal model [15]. Preliminary endoscopic OCT studies in human subjects have been reported [18–22]. Clinical studies are currently being performed by several research groups.

The objectives of this paper are to assess the feasibility of optical coherence tomography for the *in situ* imaging and screening of early pathological changes in patients with Barrett's esophagus, and to preview state-of-the-art OCT imaging techniques which promise to expand the diagnostic capabilities of this technology. Barrett's esophagus is believed to be caused by chronic gastroesophageal reflux [23]. Several studies have demonstrated that Barrett's esophagus is associated with a 30–125 times increased risk of developing adenocarcinoma. For this reason, endoscopic surveillance of Barrett's epithelium every 12–18 months is recommended [24]. Endoscopic screening currently involves random four-quadrant biopsies every 1–2 cm along the length of suspect mucosa. However, random biopsies are prone to sampling errors and small foci of carcinoma or dysplasia may be missed [25,26]. Because of

the imprecision and high cost associated with screening, new methods are being developed to assess patients at increased risk. Endoscopic ultrasound catheters have been used clinically for imaging Barrett's metaplasia with 50–100- μm resolution [27]. However, these resolutions are insufficient to identify early epithelial changes which occur in Barrett's esophagus and the premalignant changes which lead to adenocarcinoma of the esophagus.

In this study, we perform endoscopic OCT imaging of the human esophagus in patients with Barrett's esophagus. We evaluate two different OCT catheter designs, for linear and radial scanning, and assess their advantages and limitations. We investigate state-of-the-art techniques of ultrahigh-resolution and spectroscopic OCT, to explore the future potential of endoscopic OCT imaging. Finally, we propose a new balloon catheter-probe design which can enable systematic OCT imaging coverage of the esophagus for screening applications.

Materials and Methods

Optical Coherence Tomography

OCT imaging is analogous to ultrasound B-mode imaging, except that it is performed with light rather than with acoustic waves [1,2]. Figure 1 shows a schematic of the OCT system. Measurements are performed using a fiber-optic Michelson interferometer with a low coherence-length light source. Low-coherence light can be generated by sources such as compact superluminescent semiconductor diodes or ultrashort-pulse solid-state lasers. One arm of the interferometer contains a modular beam-delivery instrument that delivers and scans the light beam on the tissue and collects the reflected signal. Three OCT delivery instruments were used in this study: a linear-scanning cath-

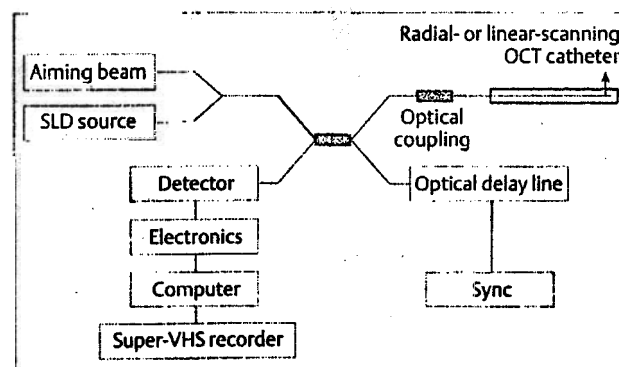


Figure 1 A schematic of the optical coherence tomography (OCT) system. Utilizing fiberoptic components, the OCT system is compact and portable, comparable in size to endoscopic ultrasound units. The system is modular in design and the sample arm of the OCT interferometer can contain a variety of beam-delivery instruments including fiberoptic radial- and linear-scanning catheter-probes for clinical endoscopic imaging, or a microscope for laboratory-based imaging of *in vitro* tissue specimens. SLD, superluminescent diode

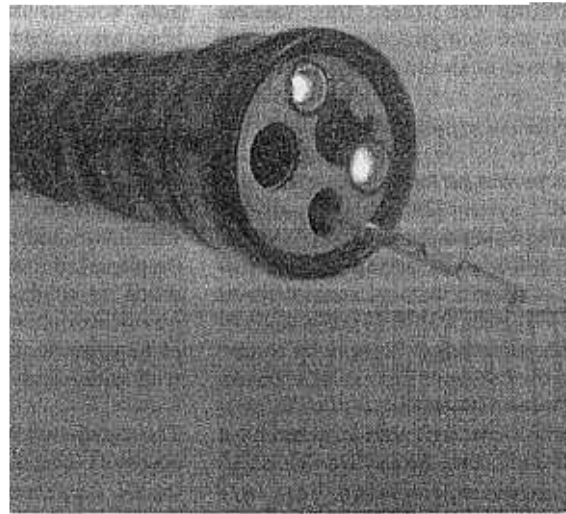
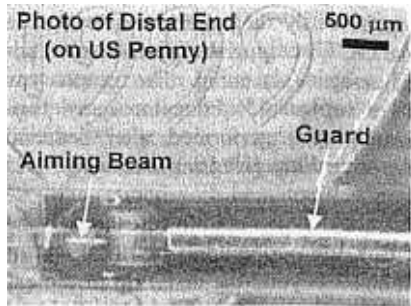
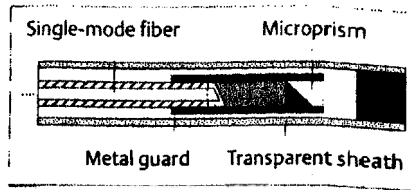


Figure 2 Endoscopic OCT catheter-probes. **A** Schematic and **B** photo of the distal end of an OCT catheter-probe. The metal cable, focusing graded-index lens, and right-angle prism are protected by a metal guard and encased within a transparent sheath. **C** The outer diameter of the catheter-probe is ~1 mm, designed to be inserted into the working channel of a standard endoscope for simultaneous endoscopic and OCT imaging.

C

eter-probe, a radial-scanning catheter-probe, and a microscope. The second arm of the interferometer is a reference arm with a mechanism for scanning the optical path length. Optical interference between the light from the sample and reference arms occurs only when the optical distances traveled match to within the coherence length of the light. By detecting and demodulating the output of the interferometer, the echo delay time and intensity of the light can be measured with extremely high accuracy and sensitivity.

Cross-sectional images of tissue are obtained by laterally scanning the optical beam and performing sequential axial measurements at different transverse positions. The beam is scanned under computer control, resulting in a two-dimensional array that represents the optical backscattering or reflection within a cross-sectional slice of the tissue specimen. The extremely high sensitivity of OCT achieves signal-to-noise ratios of 110 dB, corresponding to the detection of optical signals of 1 part in 10^{11} of the incident light.

Endoscopic OCT Catheter-Probes

A catheter-probe which is capable of focusing, scanning, and collecting a single spatial mode optical beam is a key technology for OCT imaging of internal organ systems. Small-diameter catheter-probes can be developed which can be introduced through the accessory port of a standard endoscope. This approach has the advantage of providing an endoscopic view in addition to the OCT image. In this study, we compare two OCT catheter-probe designs which use linear and radial scanning patterns [17, 19].

The OCT catheter-probe consists of an optical coupling element at its proximal end, a single-mode optical fiber running its length, and optical focusing and beam-directing elements at the distal end. The single-mode optical fiber is in a flexible hollow metal cable that is either rotated or translated with a motor drive unit at the proximal end. A

schematic and a photograph of the distal end of the OCT catheter-probes are shown in Figure 2A,B. The distal end contains a gradient-index lens and a right-angle microprism to focus and direct the beam at a 90° angle with respect to the axis of the catheter. For our studies we chose the optics for the catheter to achieve a spot size (transverse resolution) of ~13 µm and a ~2–3 mm working distance. The fiber optic cable and distal optics are protected by a sealed transparent plastic sleeve, which remains stationary as the cable and optics move inside. The catheter-probe has an outside diameter of ~1 mm and can be passed through the accessory channel of a standard endoscope as shown in Figure 2C. The radial-scan probe directs the OCT beam radially outward and scans the angle of emission rotationally to generate a "radar-like" image which is displayed in a polar plot. The linear-scan probe scans the longitudinal position of the OCT beam at a fixed angle, to generate a rectangular image of a longitudinal plane at a given angle with respect to the probe.

Clinical Endoscopic OCT Imaging System

Imaging was performed using a portable prototype clinical OCT imaging system. High-speed OCT image acquisition is important for clinical applications in order to reduce motion artifacts. Our system had an acquisition rate of 4 to 8 frames per second for 256 × 512 or 512 × 512 pixel images respectively [15]. In our studies the image acquisition rate was 4 frames per second (512-pixel image at 250 ms per image). The system used a high-speed scanning delay line which acquired 2000 axial scans per second. The axial image resolution was 16 µm in air, corresponding to ~13 µm in tissue. The low-coherence light source was a commercial high-power, broad-bandwidth source utilizing an amplified superluminescent diode. This light source operates at 1310-nm center wavelength. The incident power delivered by the OCT catheter-probe was ~5 mW. The OCT system had a display which could be either rectangular or po-

lar depending upon the imaging scan pattern. Data were recorded on Super-VHS tape and in digital form. The entire system was comparable in size to an ultrasound unit.

Ultrahigh-Resolution and Spectroscopic OCT Imaging

Imaging of *in vitro* specimens was performed using a benchtop ultrahigh-resolution OCT system [28]. This state-of-the-art system performs imaging using a femtosecond Ti:Al₂O₃ laser light source which emits ~5-fs optical pulses, corresponding to bandwidths of up to 350 nm at a center wavelength of 800 nm. The OCT system was designed to support up to 260 nm of bandwidth, achieving 1.5- μ m axial resolution in free space or ~1.1 μ m in tissue. This is an order-of-magnitude improvement in resolution compared to conventional OCT systems. An achromatic lens with a 10-mm focal length was used to focus the beam on the *in vitro* tissue specimens to achieve 5- μ m transverse resolution. This OCT system, with microscope beam delivery, was used to image *in vitro* Barrett's esophagus specimens to demonstrate the potential of ultrahigh-resolution OCT imaging.

Spectroscopic OCT imaging is an extension of ultrahigh-resolution OCT which utilizes the broad spectral bandwidth of the optical source to obtain information from the spectral content of the backscattered light [29]. Conventional OCT imaging detects the envelope of the interference signal which is generated by the reflections of light from the reference and sample arms. The amplitude of this envelope is used to display the intensity of optical backscatter from specific regions within the tissue. Spectral information can be obtained by digitizing the full interference signal and using digital signal-processing techniques.

While conventional OCT uses a one-dimensional false-color or grayscale mapping to represent the amplitude of the backscattered light, spectroscopic OCT requires a multidimensional map. In our studies, hue, saturation, luminance (HSL) color space was used. The backscattered intensity was represented by the saturation and the spectral shift was represented by the hue, keeping the luminance constant. This mapping allows the intensity and spectral shift of the backscattered light to be represented in a two-dimensional image form. Spectroscopic OCT imaging was performed on *in vitro* human esophagus specimens containing regions of normal and Barrett's epithelium. Spectroscopic OCT was investigated as a modality for improving contrast and differentiation in OCT images. Spectroscopic OCT may help identify regions of differing spectroscopic optical backscatter properties that are associated with different tissue morphologies.

Imaging Protocol

Clinical endoscopic OCT imaging of the human esophagus was performed as an adjunct to standard upper gastrointestinal endoscopy. Patients with previously diagnosed Barrett's esophagus, and with or without dysplasia, were recruited from the Gastroenterology Clinic at the West Rox-

bury Veterans Administration Medical Center, West Roxbury, Massachusetts, United States. All procedures were in compliance with human study protocols of the Committee on the Use of Humans as Experimental Subjects, MIT, Cambridge, Massachusetts, United States, and the Human Studies Internal Review Board, West Roxbury VA Medical Center, West Roxbury, Massachusetts, United States. Eight patients underwent imaging in this feasibility study (of whom two had been previously diagnosed with low-grade dysplasia). Endoscopic OCT imaging was performed in addition to routine endoscopic screening. The oropharynx was desensitized with a topical 4% lidocaine spray. Esophagogastroduodenoscopy was performed after sedation with midazolam and meperidine, given intravenously.

The disinfected OCT catheter was introduced through the accessory channel of the endoscope until the distal end of the OCT catheter extended beyond the distal tip of the endoscope and appeared in the endoscopic video field of view. Both single- and dual channel Olympus endoscopes were used in this study. Using video guidance, the OCT (Olympus America, Inc. Melville NY, USA) catheter was positioned at several normal and endoscopically abnormal-appearing sites along the length of the esophagus and OCT imaging was performed. Biopsy specimens were later acquired from OCT-imaged sites. Four quadrant biopsies were obtained every 2 cm along the esophagus; the total number of biopsies varied from patient to patient depending upon the length of the Barrett's mucosa. Continuous OCT imaging was performed at 4 frames per second using either linear- or radial-scanning OCT catheter-probes. OCT data was recorded both digitally and directly to Super-VHS video tape. Endoscopic video images were recorded directly to a second Super-VHS video tape which was synchronized to OCT video acquisition. OCT imaging was performed for approximately 5–10 minutes at multiple sites within the esophagus. An average of ~50 digital OCT images was obtained per patient.

Slightly different imaging protocols were necessary for the linear- and radial-scanning catheter-probes. The linear-scanning catheter-probe was stabilized by placing the tip in contact with the mucosal surface of the esophagus, thereby reducing motion artifacts. The positioning of the OCT imaging catheter-probe was controlled by steering the distal end of the endoscope and varying the insertion/retraction and the rotation of the catheter-probe. Special care was required to ensure that the OCT beam was emitted perpendicular to the wall of the esophagus. Imaging with the radial-scanning catheter-probe was performed by placing the probe in contact with the esophageal wall and deflating the esophagus during OCT imaging to approximate the wall around the probe. The positioning of the catheter-probe was controlled by steering the distal end of the endoscope and varying the insertion/retraction of the catheter-probe. Biopsy specimens were placed in 10% formalin for standard histological preparation and processing, and read by a gastrointestinal pathologist. Histological images were compared with corresponding OCT images.

For ex vivo ultrahigh-resolution and spectroscopic OCT imaging studies, three surgical specimens of human esophagus were used. Imaging was performed only on discarded tissue specimens. Specimens were maintained in a 0.9% saline solution and imaged with ultrahigh-resolution and spectroscopic OCT within 3 hours of resection. The tissue specimen was placed on a three-dimensional, computer-controlled, micrometer-precision translation stage. Imaging was performed using the OCT microscope beam-delivery apparatus. Immediately after OCT imaging, the specimen was marked with India ink spots to indicate the OCT image plane location. Specimens were placed in 10% formalin for at least 24 hours prior to standard histological processing. Histological slides were prepared from 5- μ m thick sections stained with hematoxylin and eosin. OCT images were compared with corresponding histological images.

Results

Endoscopic OCT was performed using both linear and radial scanning methods to evaluate scanning techniques and to demonstrate the ability to discern changes in architectural morphology associated with Barrett's esophagus. Figures 3A–C show an endoscopic video image, a biopsy histology, and a representative linear-scan OCT image of normal squamous epithelium. The OCT image (4 mm \times 2.5 mm, 512 \times 256 pixels) of normal epithelium in Figure 3C illustrates the relatively homogeneous epithelium (ep), the high-backscattering region (darker) of the lamina propria (lp), the low-backscattering muscularis mucosa (mm), the high-backscattering submucosa (sm), and the low-back-

scattering and thick muscularis propria (mp). The solid horizontal line noted above the mucosal surface was from the transparent plastic sheath of the OCT catheter. The epithelial layer in the OCT image (Figure 3C) was relatively homogeneous, correlating with the histology of a fragment of squamous epithelium (Figure 3B). The biopsy specimen was interpreted as normal squamous mucosa.

Images were also acquired from regions of Barrett's epithelium in the same patient. Figures 3D, 3E, and 3F show an endoscopic video image, a biopsy histology, and an OCT image (4 mm \times 2.5 mm, 512 \times 256 pixels) of an abnormal esophageal region. The video image reveals a finger-like projection of abnormal epithelium which appears pink. The OCT image in Figure 3F shows striking differences from those of squamous epithelium (such as Figure 3C). The uniformly layered structure has been disrupted by the presence of multiple crypt- and gland-like structures (as indicated by arrows). The presence of these gland-like morphological features is confirmed by the corresponding histological findings from the biopsy specimen. This biopsy specimen was interpreted as specialized columnar epithelium consistent with Barrett's esophagus.

Figure 4 shows two representative radial scanning OCT images. Figure 4A shows normal squamous epithelium. The epithelium appears homogeneously backscattering. The arrows in Figure 4A indicate layered structures including the lamina propria and submucosa, which is more backscattering. The image in Figure 4B is representative of regions of Barrett's epithelium. The arrow h indicates a

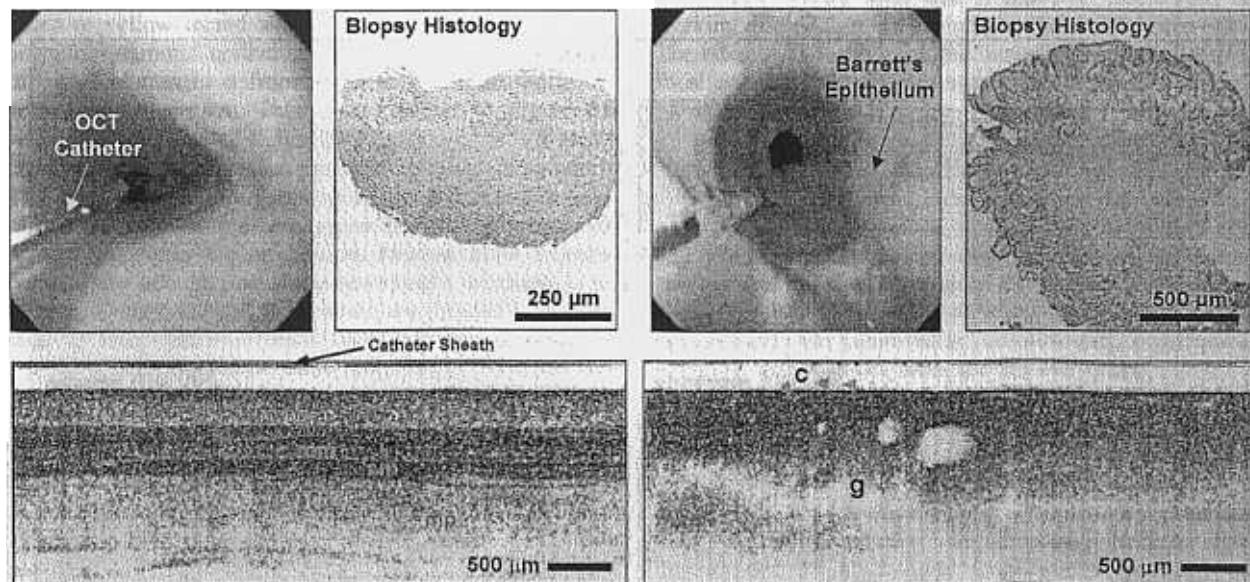


Figure 3 Clinical endoscopic OCT imaging of normal and Barrett's esophagus using linear scanning. A Endoscopic video image of normal region. B Biopsy histological image of normal squamous epithelium. C OCT image of normal squamous epithelium with relatively uniform and distinct layered structures (see Results section for details). The solid horizontal line above the mucosal

surface is the plastic sheath of the catheter. D Endoscopic video image of region showing finger-like projection of Barrett's epithelium. E Biopsy histological image of Barrett's esophagus showing characteristic specialized columnar epithelium. F OCT image of Barrett's epithelium with disruptions of layered morphology due to multiple crypt- and gland-like structures (arrows).

heterogeneous region of backscatter which appears similar to that found in metaplastic columnar epithelium. The arrows c, v, and g in Figure 4B also indicate regions of crypts, vessel, and glandular morphology, respectively.

Ultrahigh-resolution OCT was used to image specimens of human esophagus in vitro to investigate improvements in imaging. Figure 5A is an OCT image of Barrett's epithelium. The image size was 2 mm × 1 mm (1000 × 1500 pixels). The image resolution was 1.1 μm axially and 5 μm transversely. Figure 5B shows corresponding histology from the same site. Multiple crypts and glandular struc-

tures were observed along the surface. Magnified images of selected regions are shown in Figures 5C and 5D. Isolated regions of low and high optical backscatter were observed. Regions of low backscatter corresponded to fluid-filled crypts or glands. It is unclear whether individual cellular features are visible, although the localized points of high backscatter are suggestive of nuclei.

Spectroscopic OCT was performed on regions of normal and Barrett's esophagus in vitro to assess whether spectroscopic imaging could enhance image contrast or improve the differentiation of pathology. Amplitude tomograms (all previous OCT images) represent the intensity of backscatter light, while spectroscopic tomograms (Figure 6) measure the spectral content of the backscattered light. For the spectroscopic OCT images presented here, the spectral shift of the backscattered light was measured by calculating the center of gravity of the spectrum from each pixel in the image. The spectral shift is mapped to a false-color scale and plotted as hue, while the intensity of the backscattered light is plotted as saturation, with luminance kept constant. The false-color image thus provides an indication of the spectral shift of the backscattered light, as well as its intensity.

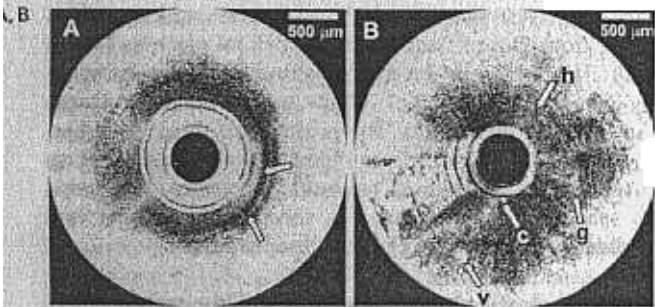


Figure 4 Clinical endoscopic OCT imaging of normal and Barrett's esophagus using radial scanning. Imaging was performed by passing the OCT catheter-probe through the working channel of a standard endoscope. **A** Representative images of normal squamous epithelium. Arrows indicate layered structures. **B** Representative images of Barrett's epithelium. Arrows indicate heterogeneous scattering regions consistent with crypts (c), glands (g), and vessels (v).

Figure 6 compares spectroscopic OCT images of normal esophagus and Barrett's esophagus. The epithelium has a green hue in the false-color image, indicating enhanced scattering of shorter wavelengths of light from this layer. Immediately below the epithelium, the lamina propria contains focal areas of red hue, indicating regions of enhanced longer-wavelength scattering. Since longer wavelengths pe-

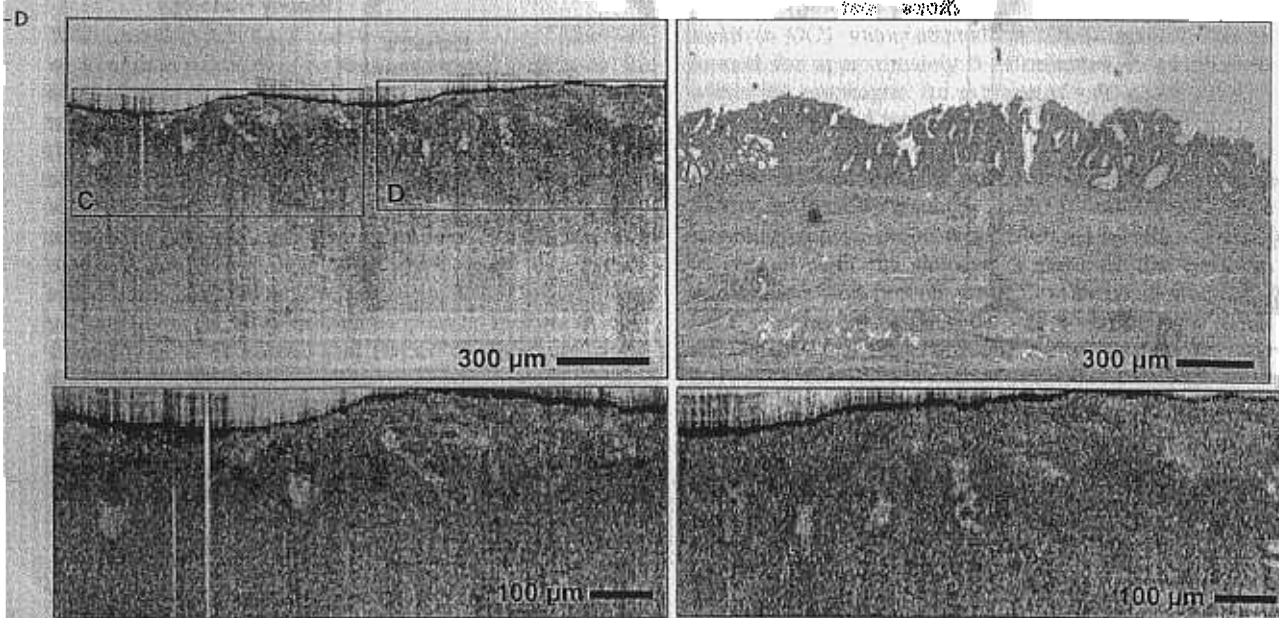


Figure 5 Ultrahigh-resolution OCT imaging of Barrett's esophagus in vitro. **A** OCT image acquired at 1.1-μm axial and 5-μm transverse resolution, illustrating multiple crypt- and gland-like structures. **B** The corresponding histological sample confirms the

architectural morphology observed in the OCT image. **C, D** Magnified regions from sites indicated in **A**. Localized regions of high optical backscatter (dark pixel clusters in image) may represent individual cell nuclei.

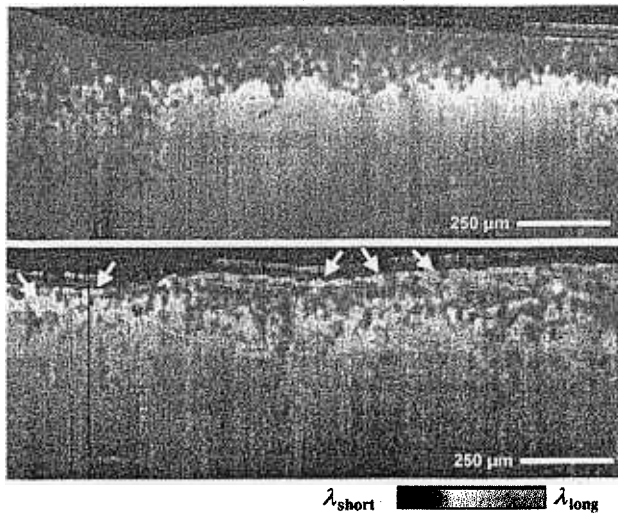


Figure 6 Spectroscopic OCT imaging. Green- and red-hue color scale indicate enhanced optical scattering of short and long wavelengths respectively. **A** Spectroscopic OCT image of transition zone between normal squamous epithelium (right) and pathologic columnar epithelium (left). For the normal epithelium, note the relatively smooth color transition from green to red with increasing depth in tissue. **B** Spectroscopic OCT image of Barrett's esophagus. The irregular epithelial morphologies from crypt- and gland-like structures are indicated by areas of red hue (enhanced long-wavelength scattering) near the surface (arrows).

penetrate more deeply into tissue, it is expected that shorter wavelengths will be scattered more from structures near the surface while longer wavelengths will be scattered more from deeper structures. Therefore, a shift of hue from green to yellow to red should occur with depth. Because normal squamous epithelium is relatively homogeneous, this gradual transition from green to yellow to red is observed in Figure 6A. This is in contrast to Figure 6B where the presence of multiple crypt and glandular structures along the surface disrupt the morphological structure. The spectroscopic tomogram in Figure 6B shows no significant degree of uniform green hue (short-wavelength scattering) within the epithelium. Instead, more frequent focal areas of red hue (long-wavelength scattering) are present. Occasional red focal areas are present at the surface, as indicated by arrows. Increased disruption of the normal squamous architectural morphology from the formation of crypts, glands, and potentially cellular structures such as increased number and size of nuclei, disrupt the normal spectroscopic scattering behavior in the spectroscopic OCT image.

Discussion

OCT enables high-resolution cross-sectional imaging of tissue morphology in situ and in real time. The ability of OCT to differentiate normal and pathologic tissue has been demonstrated by our group and others [10–14,18,21,22]. The 10–15- μm image resolution of OCT enabled the visualization of architectural morphology features such as

the normal layered structure of the epithelium vs. glandular and crypt structures associated with Barrett's esophagus. Because pinch biopsies were obtained, it was not possible to exactly orient the sectioning plane for histological investigation, as with in vitro imaging studies. Correspondence of OCT and histological findings was evaluated based on the presence or absence of architectural morphology indicating normal vs. Barrett's esophagus. There was good correlation between OCT and histological features. It should be noted, however, that OCT images display different properties from histology because the contrast in OCT images arises from optical backscattering by different tissue morphologies rather than from staining.

The image resolution of conventional OCT (10–15 μm) is sufficient to differentiate architectural but not cellular morphology. Endoscopic OCT resolution can differentiate normal from Barrett's epithelium in real time based on differences in epithelial architecture. Crypt- and gland-like structures, which disrupted the relatively uniform layers of squamous epithelium, were readily identified, enabling differentiation between normal and Barrett's epithelium. However, in this feasibility study, neither the endoscopist nor the OCT operator was blinded to the discernible Barrett's esophagus visualized endoscopically. The ability to differentiate normal from Barrett's epithelium suggests that the OCT could be used for screening applications. These findings are consistent with those of other investigations [21,22].

Another aim of our study was to evaluate linear- and radial-scanning OCT catheter-probes and to assess their advantages and limitations. In OCT imaging catheter-probes, the focused beam spot size (transverse resolution) and working distance are determined by the distal micro-optics. The beam is in focus when the tissue is positioned near the focal position of the beam within the depth of field. The linear scan pattern was used in clinical gastrointestinal imaging studies reported in the literature [19,21]. Linear-scanning OCT images were displayed in Cartesian (rectangular) coordinates, whereas images acquired with the radial-scanning catheter-probe were displayed in polar (circular) coordinates. The linear scanning approach has the advantage that the pixel spacing in the transverse direction is always uniform. This contrasts with the radial imaging approach where the transverse (circumferential) pixel spacing increases with distance from the catheter-probe.

To image with the linear-scan catheter-probe design, the distal end was positioned against the wall of the esophagus. Placing the catheter in contact with tissue not only fixed the distance to the tissue, but also helped stabilize the catheter-probe position during cardiac or respiratory movements. Since the OCT imaging was performed in a plane oriented at a particular angle, the catheter-probe had to be rotated to ensure that the imaging plane was positioned in the correct direction to intercept the wall of the esophagus. This added an additional degree of freedom that had to be controlled during imaging. The rectangular OCT images were freer from distortion and appeared higher in quality

than radial-scanning OCT images with comparable pixel densities. The longitudinal orientation of the OCT image plane was well suited for imaging structures such as the gastric junction, but provided poor coverage of the surface of the esophagus, since multiple views were required.

The second OCT catheter-probe design performed radial scanning. The radial-scanning catheter-probe was similar to an earlier design developed for OCT imaging of the gastrointestinal tract system in animals [17]. This scan design was used in clinical gastrointestinal imaging studies reported in the literature [20,22]. The radial scanning method is analogous to that used in intravascular ultrasound catheters which contain a rotating distal ultrasonic transducer. The radial-scanning catheter-probe is well suited for imaging small-diameter lumens (of the order of a few mm) such as human arteries or the gastrointestinal tract of animals. However, for large-diameter lumens such as the human esophagus, it is difficult to position and stabilize the radial-imaging catheter-probe in the center of the lumen. Movements of the esophagus or endoscope resulted in motion artifacts and variations in the focus position. If radial imaging is performed with the catheter-probe decentered in the esophagus and near the mucosal surface, only a small sector of the 360° scan range is in focus. Therefore, the images shown in Figure 4 were obtained by collapsing the esophagus around the OCT catheter. This also stabilized the position of the esophagus relative to the catheter-probe. However, folds in the esophagus developed around the probe so that the full circumference could not be visualized with a single probe placement, and the OCT probe could not be viewed endoscopically. Finally, imaging with the radial-scanning probe requires that the image be displayed in a polar plot. The transverse pixel spacing (along the circumference) is not constant, but increases with distance from the probe. Thus, the radial OCT images become progressively coarser when large-diameter lumens are scanned.

In order to systematically image the lumen, it will be necessary to develop new OCT imaging probes that integrate imaging and position stabilization. The radial-scanning catheter-probe can image the entire cross-section of the esophagus, provided it is positioned near the center of the lumen and the esophagus is insufflated to a diameter sufficient to avoid folds. One approach is to use radial scanning in conjunction with a balloon. Balloon catheters are commonly used for dilation of strictures and have been used in photodynamic therapy, where they expand and stabilize the esophagus to facilitate uniform delivery of optical radiation. A schematic of one type of proposed OCT balloon catheter-probe is shown in Figure 7. The balloon catheter integrates the radial-scanning catheter shown in Figure 2 with a wire-guided esophageal balloon-dilation catheter. The balloon stabilizes the position of the OCT catheter-probe in the center of the esophagus and sets the correct working distance so that the OCT beam is focused on the esophagus. In addition, the balloon also insufflates the esophagus to remove folds and allow imaging of the full circumference. Imaging can be performed at successive

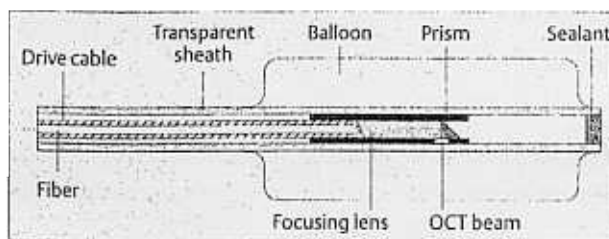


Figure 7 A schematic of the OCT balloon catheter-probe. Dilation of the balloon within the esophagus stabilizes catheter position, maintains a fixed optical working distance, and enables three-dimensional imaging. A spiral scanning technique could be used for three-dimensional OCT balloon catheter-probe imaging and could enable systematic imaging of the esophagus

longitudinal positions along the esophagus by varying the longitudinal position of the optical probe within the balloon or by retracting the entire balloon device. Alternatively, imaging can be performed by scanning the OCT beam in a spiral pattern, analogous to spiral computed tomography. Computer algorithms could then be used to reconstruct the three-dimensional structure of the mucosa.

Current acquisition rates of 4 frames per second were sufficient for real-time endoscopic imaging. However, if systematic coverage of the esophagus is required, the amount of data increases dramatically. Radial-scanning catheter-probes can image the esophagus surface; however, because the area is large, image-acquisition times increase. If the esophagus is 10 mm in diameter, the circumference is 31.4 mm and imaging with a transverse resolution of 15 μm requires a minimum of $2 \times (31.4 \text{ mm}/15 \text{ mm}) = \sim 4000$ pixels. Current OCT systems, at 4–8 frames per second (or 2000–4000 transverse pixels per second), would require 1–2 seconds to image the esophagus circumference. Multiple images of the esophagus at different longitudinal positions would be necessary to cover a given area. Alternatively, a spiral scan pattern could be used. In order to scan a 15-cm length with cross-sectional images separated by 2 mm, 75 images are required and the acquisition time would be 75–150 seconds. These times would still be feasible for screening; however, if higher resolutions are required, then the image-acquisition times would increase proportionally. For example, imaging with 5-μm resolution requires $2 \times (31.4 \text{ mm}/5 \text{ μm}) = \sim 12000$ pixels for a single cross-sectional plane, producing a threefold increase in image acquisition time. Thus, OCT systems with higher image-acquisition rates would be required. Finally, computer monitors have insufficient resolution to display a full image, so it would be necessary to pan and zoom in on areas of interest, or to unfold the normal circular view of the esophagus into a series of sector views.

One major unresolved question is the ability of OCT to differentiate high-grade and low-grade dysplastic changes that occur in conjunction with Barrett's esophagus. Because many signatures of dysplasia are manifest on a sub-cellular rather than an architectural morphology level,

higher-resolution imaging may be required. Ultrahigh-resolution OCT has achieved subcellular resolution in vivo including imaging in an amphibian animal model [28]. However, cell sizes in developmental biology models are larger than in human tissues. In this study, ultrahigh-resolution OCT imaging of specimens *ex vivo* showed clearer differentiation of architectural morphology associated with Barrett's esophagus than did lower-resolution OCT imaging. Spectroscopic OCT imaging of specimens *ex vivo* showed clear differences in the spectral content of backscattered light from normal vs. Barrett's esophagus. The use of spectroscopic features provides another approach for enhancing contrast between different tissue pathologies. Light-scattering measurements have recently emerged as a potentially powerful approach for characterizing nuclear size by examining spectral features which are dependent upon the size of the scatterers [30–32]. Spectroscopic OCT can provide spectroscopically resolved cross-sectional images and might be used to extract information on cellular features. However, if successful, spectroscopic techniques would be a lower-cost and lower-complexity solution for grading dysplasia than OCT.

OCT has the potential to be integrated into several areas of upper gastrointestinal endoscopy. OCT may be used as an adjunct to endoscopy for screening and surveillance of Barrett's esophagus. Barrett's esophagus is usually visible endoscopically; however, OCT might be used in situations where endoscopic visualization is difficult, such as to detect short-segment Barrett's, or as a follow-up to photodynamic therapy to detect residual islands of Barrett's pathology [33].

OCT may also be used in the context of endoscopic mucosal resection of superficial, early-stage neoplasms. Endoscopic ultrasound with 15-MHz probes has been used to determine the depth of tumor invasion; however, resolutions are limited, and in one study correct depth of tumor invasion was determined in only 67% of patients [34]. The higher resolution of OCT may prove useful for accurately determining whether there is submucosal involvement of a tumor. OCT may also be used intraoperatively to provide surgical guidance during mucosal resection and to provide feedback on the location of the tumor margin.

OCT could be useful for screening patients with gastroesophageal reflux disease for Barrett's esophagus. The use of a balloon-imaging catheter-probe is especially applicable for screening. In this case, if OCT can be used to systematically image the esophagus, it could be used independently of endoscopy. Endoscopic OCT could be performed by a small transoral or transnasal catheter-probe. This would have the advantage of enabling "first-look" screening to be performed without the need for conventional endoscopy. Screening could be performed without patient sedation, without the need for special facilities, and at lower cost than conventional endoscopy. If OCT screening is positive, then follow-up endoscopy could be performed.

In the context of surveillance of patients with Barrett's for high-grade dysplasia and adenocarcinoma, the most intriguing application of OCT would be to direct excisional biopsy, to reduce sampling errors. One can envision new OCT imaging probes which integrate OCT imaging with pinch biopsy to provide a real-time "first look" at pathology prior to excision and processing of a specimen. Diagnosis and treatment decisions would still be made using the gold standard of histopathology; however the number of biopsies and the sampling error would be reduced. Further investigations are required to assess the potential for conventional-resolution, ultrahigh-resolution, or spectroscopic OCT to grade dysplasia. At present, there are limitations in the clinical use of ultrahigh-resolution and spectroscopic OCT imaging, because these systems utilize femtosecond lasers which are still relatively large, complex, and costly. Advances in technology are required to make ultrahigh-resolution OCT practical for the clinical environment. However in the future, clinical OCT instruments with image resolutions of 1–2 μm as well as spectroscopic imaging capabilities should be possible.

Acknowledgments

We would like to acknowledge the contributions of Pei-Lin Hsiung, Tony Ko, Christian Chudoba, Ingmar Hartl, and Ravi Ghanta. We also thank Drs Uwe Morgner, Franz Kaertner, and Erich Ippen for the development of the ultrahigh-resolution and spectroscopic OCT systems. We appreciate the laboratory contributions of Christine Jesser and Kathleen Saunders. We also thank former group members, Drs Brett Bouma and Gary Tearney, currently at the Wellman Laboratory, Massachusetts General Hospital, for their contributions.

This research was supported in part by the National Institutes of Health, Contracts NIH-9-RO1-CA75289-03 (JGF), NIH-9-RO1-EY11289-14 (JGF), NIH-RO1-AR44812-02 (MEB), and NIH-1-R29-HL55686-02A1 (MEB), the Medical Free Electron Laser Program, Office of Naval Research Contract N000014-97-1-1066 (JGF and MEB), the Boston VA Health Care System, and the Air Force Palace Knight Program (SAB).

References

- 1 Huang D, Swanson EA, Lin CP, et al. Optical coherence tomography. *Science* 1991; 254: 1178–1180
- 2 Fujimoto JG, Pitris C, Boppart SA, Brezinski ME. Optical coherence tomography, an emerging technology for biomedical imaging and optical biopsy. *Neoplasia* 2000; 2: 9–25
- 3 Hee MR, Izatt JA, Swanson EA, et al. Optical coherence tomography of the human retina. *Arch Ophthalmol* 1995; 113: 325–332
- 4 Puliafito CA, Hee MR, Lin CP, et al. Imaging of macular diseases with optical coherence tomography. *Ophthalmology* 1995; 102: 217–229
- 5 Puliafito CA, Hee MR, Schuman JS, Fujimoto JG. Optical coherence tomography of ocular diseases. Thorofare, New Jersey Slack: 1996

- ⁶ Schmitt JM, Knuttel A, Yadlowsky M, Eckhaus MA. Optical coherence tomography of a dense tissue – statistics of attenuation and backscattering. *Phys Med Biol* 1994; 39: 1705–1720
- ⁷ Schmitt JM, Yadlowsky M, Bonner RF. Subsurface imaging of living skin with optical coherence tomography. *Dermatology* 1995; 191: 93–98
- ⁸ Fujimoto JG, Brezinski ME, Tearney GJ, et al. Optical biopsy and imaging using optical coherence tomography. *Nat Med* 1995; 1: 970–972
- ⁹ Brezinski ME, Tearney GJ, Bouma BE, et al. Optical coherence tomography for optical biopsy: properties and demonstration of vascular pathology. *Circulation* 1996; 93: 1206–1213
- ¹⁰ Izatt JA, Kulkarni MD, Hsing-Wen W, et al. Optical coherence tomography and microscopy in gastrointestinal tissues. *IEEE J Selected Topics Quantum Electronics* 1996; 2: 1017–1028
- ¹¹ Tearney GJ, Brezinski ME, Southern JF, et al. Optical biopsy in human gastrointestinal tissue using optical coherence tomography. *Am J Gastroenterol* 1997; 92: 1800–1804
- ¹² Tearney GJ, Brezinski ME, Southern JF, et al. Optical biopsy in human pancreatobiliary tissue using optical coherence tomography. *Dig Dis Sci* 1998; 43: 1193–1199
- ¹³ Kobayashi K, Izatt JA, Kulkarni MD, et al. High-resolution cross-sectional imaging of the gastrointestinal tract using optical coherence tomography: preliminary results. *Gastrointest Endosc* 1998; 47: 515–523
- ¹⁴ Pitris C, Jesser C, Boppart SA, et al. Feasibility of optical coherence tomography for high resolution imaging of human gastrointestinal tract malignancies. *J Gastroenterol* 1999; 35: 87–92
- ¹⁵ Tearney GJ, Brezinski ME, Bouma BE, et al. In vivo endoscopic optical biopsy with optical coherence tomography. *Science* 1997; 276: 2037–2039
- ¹⁶ Boppart SA, Bouma BE, Pitris C, et al. Forward-imaging instruments for optical coherence tomographic imaging. *Opt Lett* 1997; 22: 1618–1620
- ¹⁷ Tearney GJ, Boppart SA, Bouma BE, et al. Scanning single-mode fiber optic catheter-endoscope for optical coherence tomography. *Opt Lett* 1997; 21: 1–3
- ¹⁸ Sergeev AM, Gelikonov VM, Gelikonov GV, et al. In vivo endoscopic OCT imaging of precancer and cancer states of human mucosa. *Opt Express* 1997; 1: 432–440
- ¹⁹ Bouma BE, Tearney GJ. Power-efficient nonreciprocal interferometer and linear-scanning fiber-optic catheter for optical coherence tomography. *Opt Lett* 1999; 24: 531–533
- ²⁰ Rollins AM, Ung-arunyawee R, Chak A, et al. Real-time in vivo imaging of human gastrointestinal ultrastructure by use of endoscopic optical coherence tomography with a novel efficient interferometer design. *Opt Lett* 1999; 24: 1358–1360
- ²¹ Bouma BE, Tearney GJ, Compton CC, Nishioka NS. High-resolution imaging of the human esophagus and stomach in vivo using optical coherence tomography. *Gastrointest Endosc* 2000; 51: 467–474
- ²² Sivak MV Jr, Kobayashi K, Izatt JA, et al. High-resolution endoscopic imaging of the gastrointestinal tract using optical coherence tomography. *Gastrointest Endosc* 2000; 51: 474–479
- ²³ Phillips RW, Wong RKH. Barrett's esophagus: natural history, incidence, etiology, and complications. *Gastroenterol Clin N Am* 1991; 2: 791–815
- ²⁴ Sampliner RE. Practice guidelines on the diagnosis, surveillance, and therapy of Barrett's esophagus. The Practice Parameters Committee of the American College of Gastroenterology. *Am J Gastroenterol* 1998; 93: 1028–1032
- ²⁵ Falk GW, Rice TW, Goldblum JR, Richter JE. Jumbo biopsy forceps protocol still misses unsuspected cancer in Barrett's esophagus with high-grade dysplasia. *Gastrointest Endosc* 1999; 49: 170–176
- ²⁶ Axon AT. Cancer surveillance in ulcerative colitis – a time for reappraisal. *Gut* 1994; 35: 587–589
- ²⁷ Adrain AL, Ter H-C, Cassidy MJ, et al. High-resolution endoluminal sonography is a sensitive modality for the identification of Barrett's metaplasia. *Gastrointest Endosc* 1997; 46: 147–151
- ²⁸ Drexler W, Morgner U, Kartner FX, et al. In vivo ultrahigh-resolution optical coherence tomography. *Opt Lett* 1999; 24: 1221–1223
- ²⁹ Morgner U, Drexler W, Kartner FX, et al. Spectroscopic optical coherence tomography. *Opt Lett* 2000; 25: 111–113
- ³⁰ Perelman LT, Backman V, Wallace M, et al. Observation of periodic fine structure in reflectance from biological tissue: a new technique for measuring nuclear size distribution. *Phys Rev Lett* 1998; 8: 627–630
- ³¹ Backman V, Gurjar R, Badizadegan K, et al. Polarized light scattering spectroscopy for quantitative measurement of epithelial cellular structures in situ. *IEEE J Selected Topics Quantum Electronics* 1999; 5: 1019–1026
- ³² Backman V, Wallace M, Perelman LT, et al. Detection of preinvasive cancer cells. Early-warning changes in precancerous epithelial cells can now be spotted in situ. *Nature* 2000; 406: 35–36
- ³³ Biddlestone LR, Barham CP, Wilkinson SP, et al. The histopathology of treated Barrett's esophagus: squamous reepithelialization after acid suppression and laser and photodynamic therapy. *Am J Surg Pathol* 1998; 22: 239–245
- ³⁴ Akahoshi K, Chijiwa W, Hamada S, et al. Pretreatment staging of endoscopically early gastric cancer with a 15 MHz ultrasound catheter probe. *Gastrointest Endosc* 1998; 48: 542–545

Corresponding Author

Jacques Van Dam, M.D., Ph.D.

Division of Gastroenterology & Hepatology
 Stanford University Medical Center
 300 Pasteur Drive – Room H1121
 Stanford, California 94305-5202
 United States

Fax: +1-650-498-4302

Submitted: 13 June 2000

Accepted after Revision: 21 August 2000